Supplementary Materials

Carbon Doping of Hexagonal Boron Nitride Porous Materials toward CO_2 Capture

Siru Chen[a,1], Pan Li[a, b, 1], Shutao Xu[a,c], Xiulian Pan[a], Qiang Fu[a,*], Xinhe Bao[a,b]

[a] *State Key Laboratory of Catalysis, iChEM, Dalian Institute of Chemical Physics, the Chinese Academy of Sciences, Dalian 116023, P.R. China*

[b] *Department of Chemical Physics, University of Science and Technology of China, Hefei 230026, P.R. China*

[c] *National Engineering Laboratory for Methanol to Olefins, Dalian National Laboratory for Clean Energy, Dalian Institute of Chemical Physics, the Chinese Academy of Sciences, Dalian 116023, P.R. China*

Email: qfu@dicp.ac.cn; Tel: 0086-411-84379253

Table S1. Chemical compositions of BN and BCN samples

Sample	Elemental analysis[a] (wt. %)				ICP[b] (wt. %)
	C	N	O	H	B
BCN(1:4)	10.3	34.5	21.8	2.10	20.5
BN(1:4)	1.00	26.6	16.0	1.47	32.3
BCN(1:2)	12.1	42.0	14.9	1.66	20.1
BN(1:2)	0.72	44.7	6.48	0.90	35.0
BCN(2:1)	11.0	40.1	12.9	1.39	24.8
BN(2:1)	0.56	41.9	7.03	0.99	35.0

a) the elemental analysis is suitable for light elements like carbon, hydrogen, nitrogen, oxygen, and sulfur which can be vaporized by heating the sample drastically to 1350 ^{o}C and are detected by TCD (for N element) or IR (for C, H, O) detector. For boron it is not possible to measure its content using elemental analysis since it cannot be vaporized at the given condition; b) ICP is suitable for primary metallic elements, and boron is one of the non-metal element that can be detected by ICP analysis.

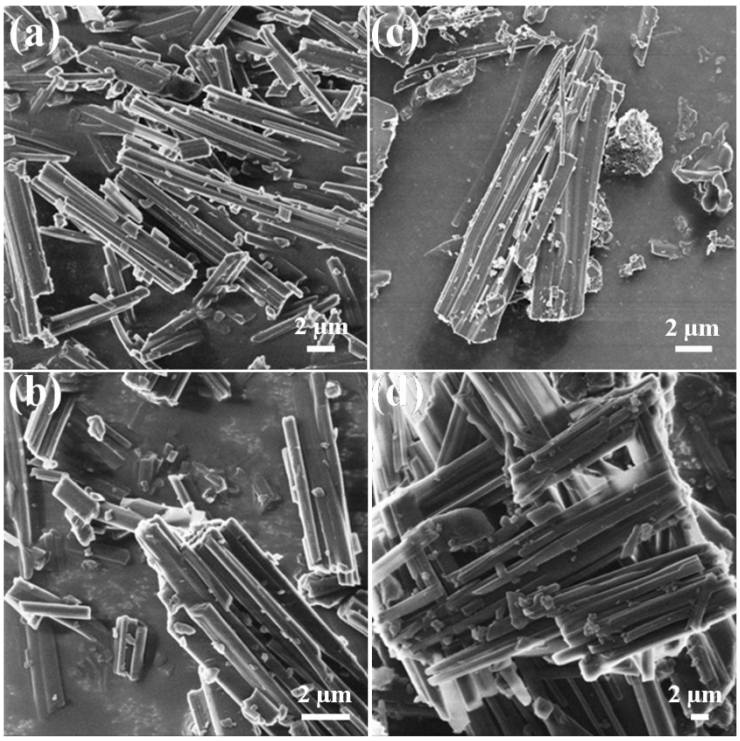

Figure S1 HIM images of BN and BCN samples: (a) BCN (2:1), (b) BCN (1:4), (c) BN (2:1), and (d) BN (1:4).

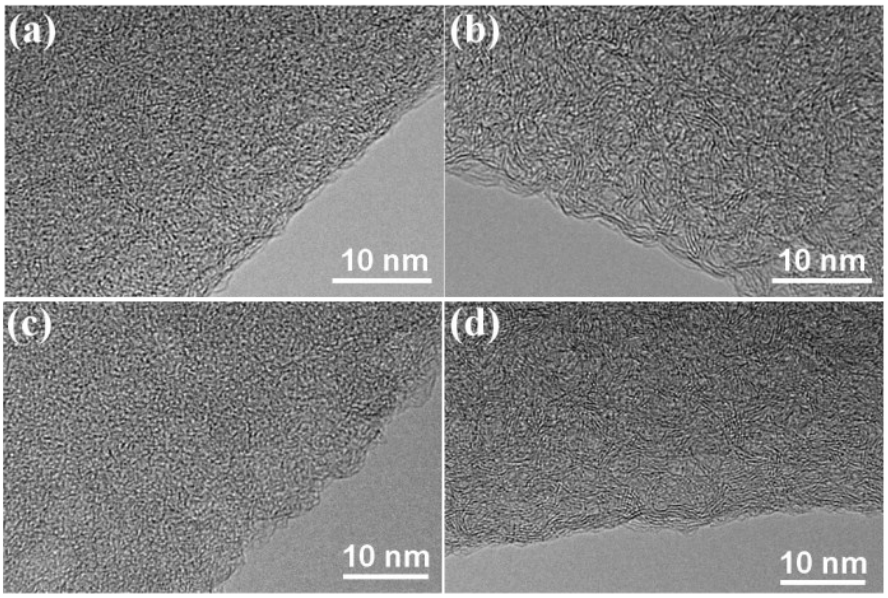

Figure S2 HRTEM images of BN and BCN samples: (a) BCN (2:1), (b) BN (2:1), (c) BCN (1:4), and (d) BN (1:4).

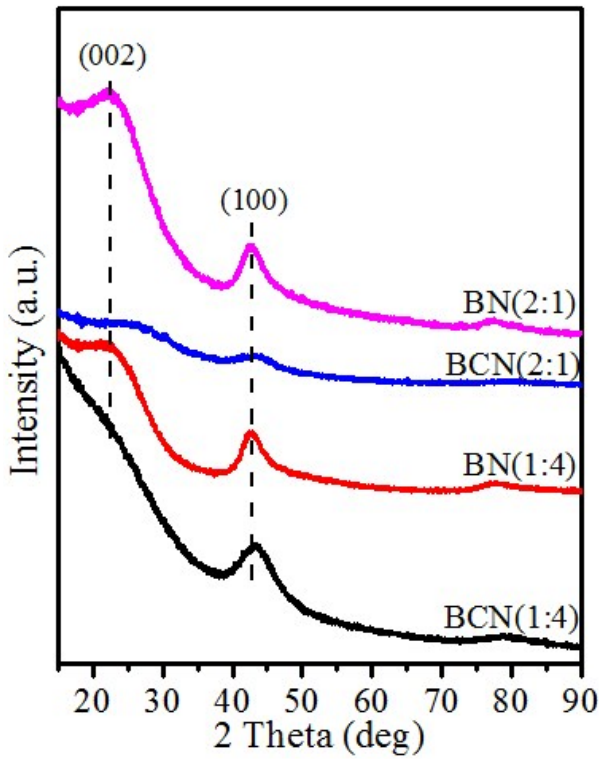

Figure S3 XRD patterns of the BN and BCN samples.

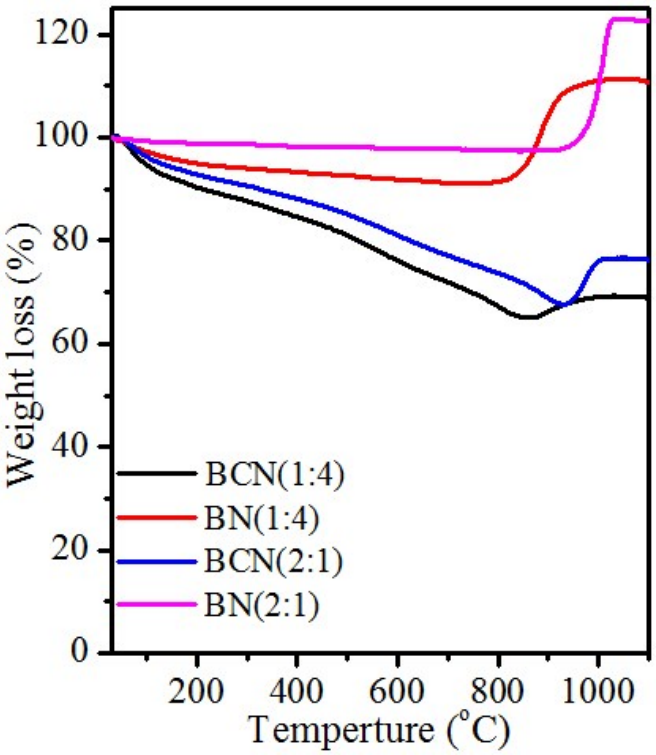

Figure S4 TG plots of the BN and BCN samples. The samples were heated in air from room temperature to 1100 °C with a heating rate of 10 °C/min.

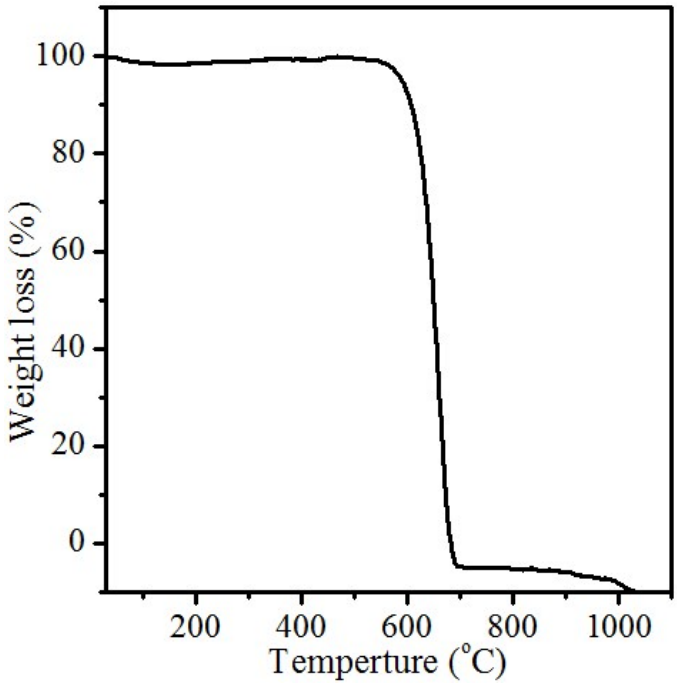

Figure S5 TG plot of activated carbon material (Ketjen Black EC-600JD). The sample was heated in air from room temperature to 1100 °C with a heating rate of 10 °C/min.

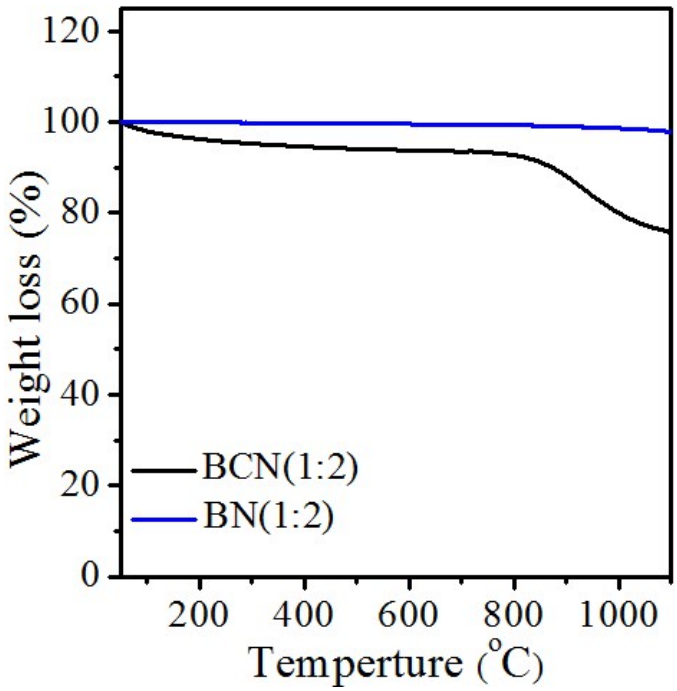

Figure S6 TG plots of the BN(1:2) and BCN(1:2) samples. The samples were heated in Ar from room temperature to 1100 °C with a heating rate of 10 °C/min.

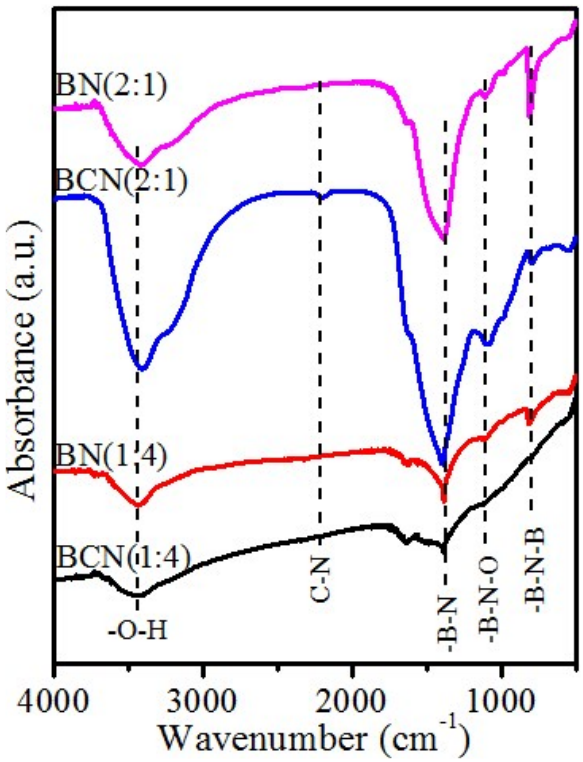

Figure S7 FTIR spectra of BN and BCN samples.

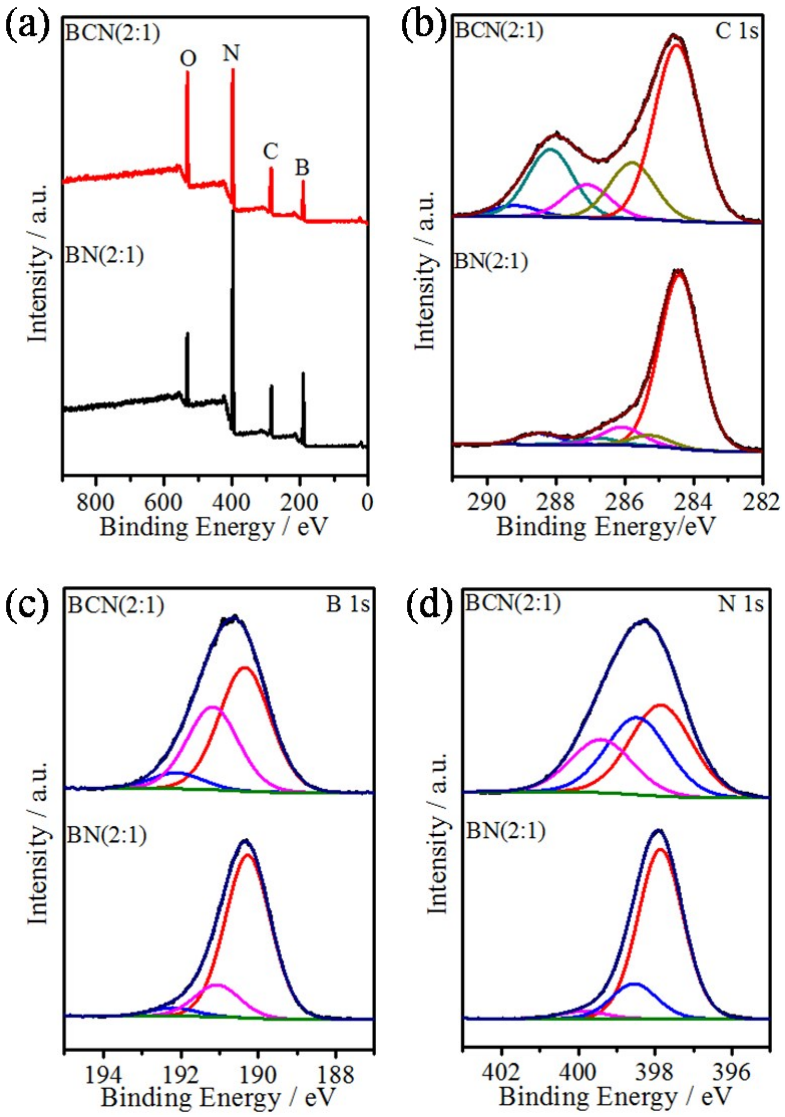

Figure S8 XPS survey (a), C 1s (b), B 1s (c), and N 1s (d) spectra of BN (2:1) and BCN (2:1) samples.

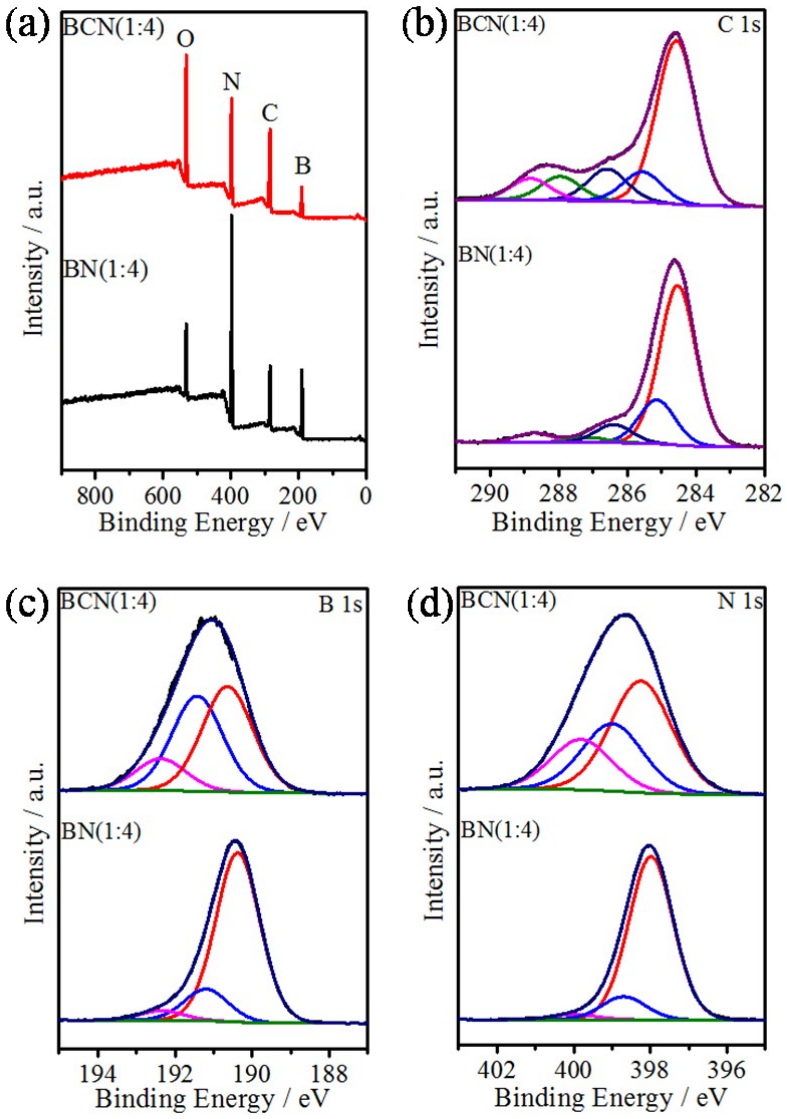

Figure S9 XPS survey (a), C 1s (b), B 1s (c), and N 1s (d) spectra of BN (1:4) and BCN (1:4) samples.

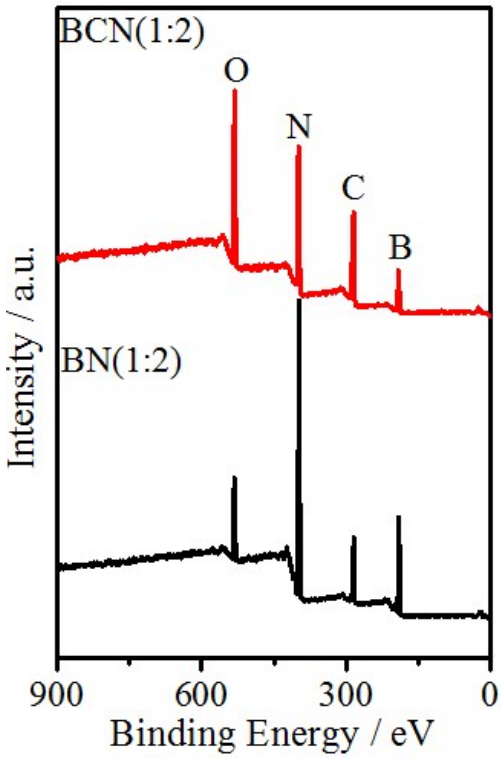

Figure S10 XPS survey spectra of BN (1:2) and BCN (1:2) samples.

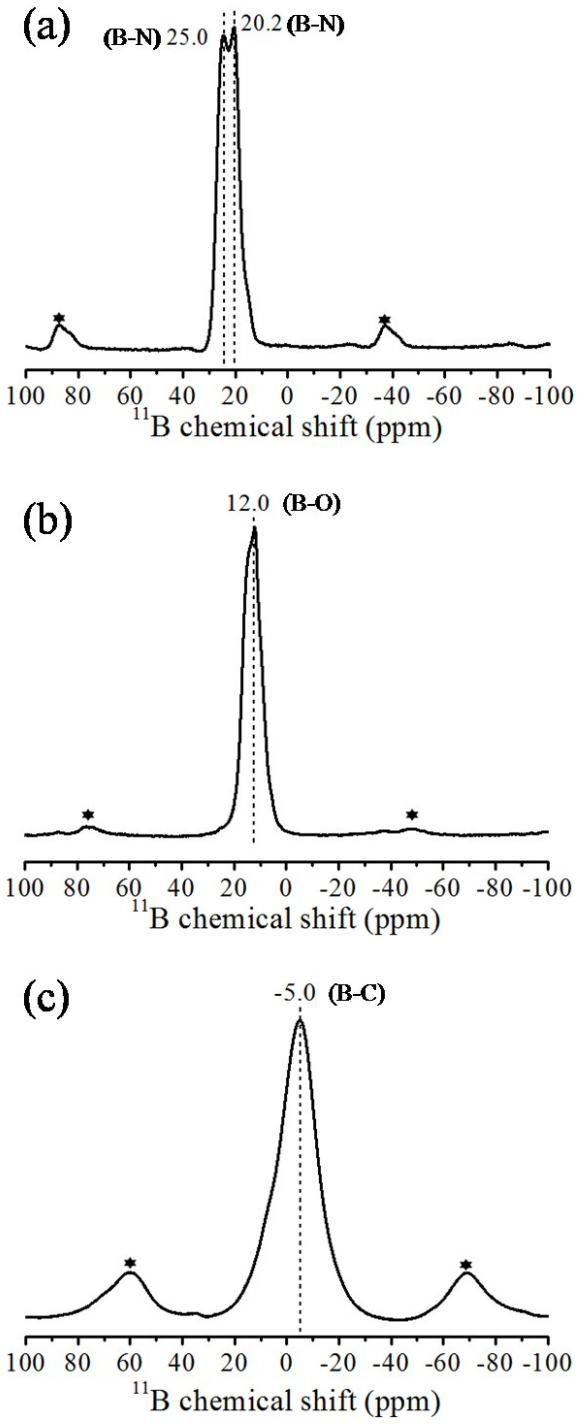

Figure S11 ^{11}B solid state MAS NMR spectra of commercial h-BN material (a), commercial B_2O_3 powder (b), and commercial B_4C powder (c). * denotes spinning side band.

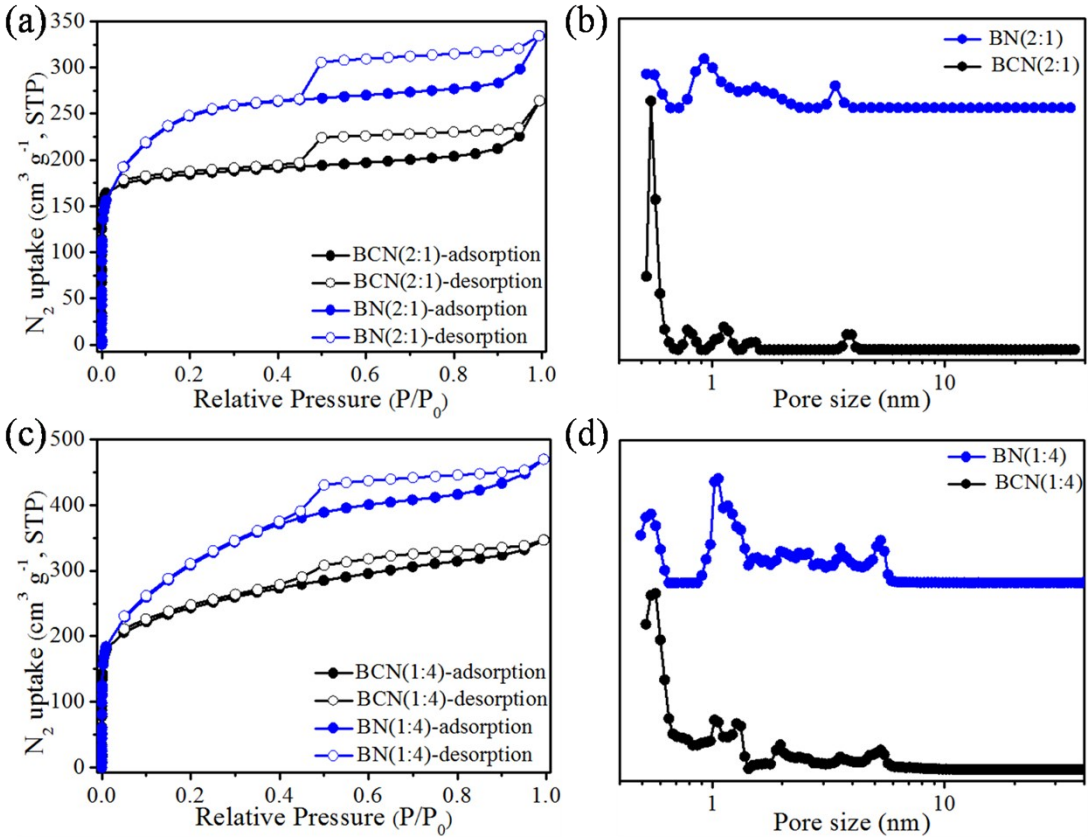

Figure S12 Nitrogen adsorption-desorption isotherms of BN and BCN samples at 77 K: BN (1:2) and BCN (1:2) samples (a), BN (4:1) and BCN (4:1) samples (c); the corresponding pore size distribution curves of the BN and BCN samples: BN (1:2) and BCN (1:2) samples (b), BN (4:1) and BCN (4:1) samples (d).

Calculation of heats of adsorption

Isosteric heat of adsorption (Q_{st}) for all the porous BN and porous BCN samples were calculated using the CO_2 sorption isotherms measured at 273 and 298 K based on the Clausius-Clapeyron equation using the ASiQwin software installed in Quantachrome Autosorb-iQ2 instruments. Clausius-Clapeyron equation is in the form:

$$ln\left(\frac{p_2}{p_1}\right) = \frac{Q_{\mathrm{st}}}{R}\left(\frac{1}{T_1} - \frac{1}{T_2}\right)$$

where Q_{st} is the isosteric heats of adsorption, Ti represents a temperature at which an isotherm i is measured, p_i represents a pressure at which a specific equilibrium adsorption amount is reached at T_i, R is the universal gas constant (8.314 J K^{-1} mol^{-1}).

High-pressure CO_2 uptake of BN and BCN samples

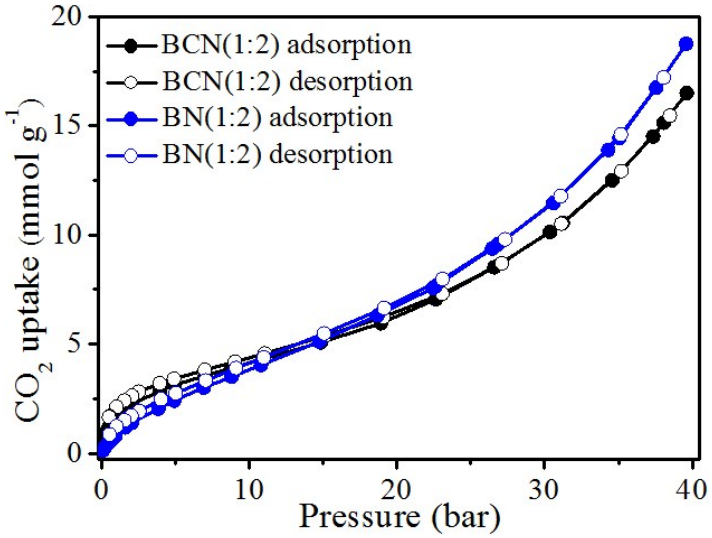

Figure S13 High-pressure CO_2 uptake of BN(1:2) and BCN(1:2) samples at 298 K.

IAST Selectivity Analysis

Ideal Adsorption Solution Theory (IAST)

We used the IAST of Myers and Prausnitz [1] along with the single-component adsorption isotherm fits to determine the molar loadings in the mixture for specified partial pressures in bulk phases. The excess adsorption data for pure CO_2, N_2 measured at 298 K, were first converted to absolute loadings using the Peng-Robinson equation of state for estimation of the fluid densities. The absolute component loadings at 298 K were fitted using the single-site Langmuir-Freundlich model. The fitted constants are listed in Table S2.

The single-site Langmuir-Freundlich model can be expressed as follows:

$$N = A_1 \times \frac{b_1 p^{c_1}}{1 + b_1 p^{c_1}}$$

Where A_1 is saturation capacity and b_1, c_1 are constant.

IAST predicts the mixture adsorption equilibriums using single-component adsorption isotherms is defined by

$$S_{CO_2/N_2} = \frac{q_1/q_2}{p_1/p_2}$$

where q_1 and q_2 are the CO_2 and N_2 uptake capacities (mmol g^{-1}), respectively; p_1 and p_2 are the specified partial pressure of CO_2 and N_2, respectively.

Table S2. Parameters of single-site Langmuir-Freundlich model by fitting absolute adsorption of pure CO_2 and N_2 at 298 K.

Adsorbent	Adsorbate	A_1 (mmol g^{-1})	b_1 (kPa^{-1})	c_1	R^2
BN(1:2)	CO_2	9.1164	0.02793	0.70004	0.9999
	N_2	2.3666	0.00118	1.03232	0.9999

Adsorbent	Adsorbate	A_1 (mmol g^{-1})	b_1 (kPa^{-1})	c_1	R^2
BCN(1:2)	CO_2	12.022	0.00223	0.85984	0.9999
	N_2	30.791	1.5638E-6	1.16939	0.9989

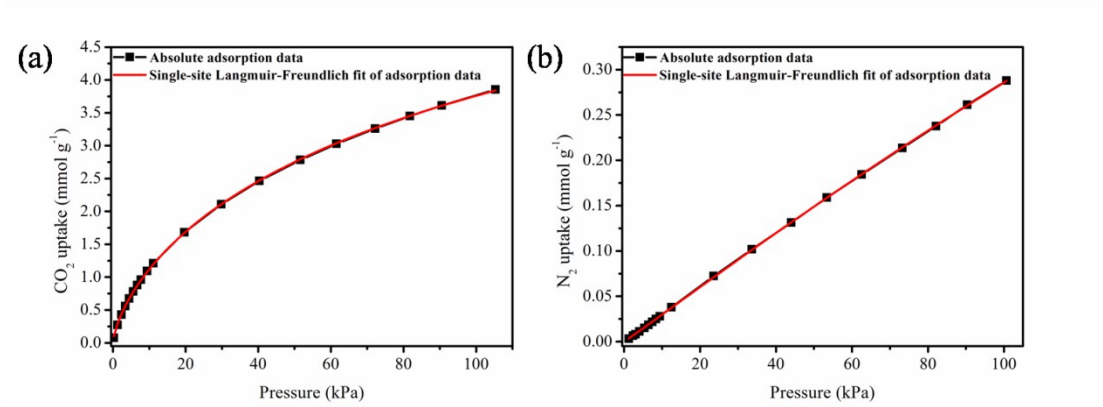

Figure S14. Single-site Langmuir-Freundlich fit of the (a) CO_2 adsorption data and (b) N_2 adsorption data on BCN (1:2) at 298 K. The corresponding fitted parameters were used for calculation of the IAST data.

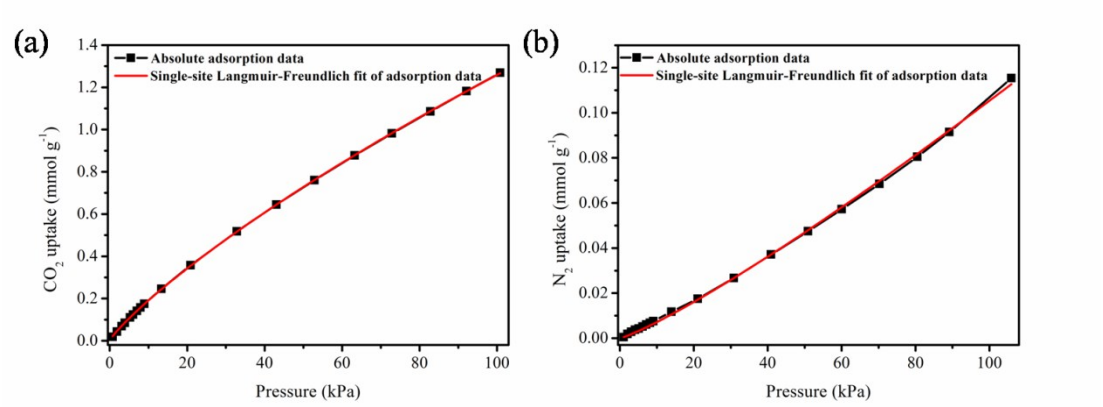

Figure S15. Single-site Langmuir-Freundlich fit of the (a) CO_2 adsorption data and (b) N_2 adsorption data on BN (1:2) at 298 K. The corresponding fitted parameters were used for calculation of the IAST data.

Table S3. Summary of textual properties and CO_2 capture performances of BN (1:2) and BCN (1:2) samples in comparison to results reported in literatures from porous materials.

Samlpe	S_{BET}[a] (m^2/g)	CO_2 uptake[b] (mmol/g)	IAST CO_2/N_2	Reference
BCN(1:2)	874	3.85	74	This work
BN(1:2)	1132	1.27	18	This work
mJUC-160-900	940	3.50	29	[2]
ZIF-69	950	2.23	20	[3]
ZIF-8	1025	-	23	[4]
Mg-MOF-74	1800	8.27	44	[5]
Ni-MOF-74	936	7.14	30	[6, 7]
SNU-100-Co	1000	3.80	27	[8]
PCN-88	3308	4.2	18	[9]
Zeolite 13X	488	4.2	100	[10]
Zeolite 4A	-	-	19	[11]
NaX zeolite	-	-	152	[12]
h-BN nanosheet	235	0.45	26.3	[13]
BN pellet	1900	1.1	-	[14]
BN-200	1016	0.6	-	[15]
Porous carbon AC-2–635	381	3.86	21	[16]
Porous carbon ATS-2-700	1330	3.3	15	[17]

a) Brunauer–Emmett–Teller (BET) specific surface area; b) CO_2 uptake at 298 K, 1bar.

Reference

1 A.L. Myers and J.M. Prausnitz, *AIChE J.*, 1965, **11,** 121.

2 Y. Pan, M. Xue, M. Chen, Q. Fang, L. Zhu, V. Valtchev and S. Qiu, *Inorg. Chem. Front.*, 2016, **3,** 1112.

3 H. Alawisi, B. Li, Y. B. He, H. D. Arman, A. M. Asiri, H. L. Wang and B. L. Chen, *Cryst. Growth Des*., 2014, **14**, 2522.

4 Z. Zhang, S. Xian, Q. Xia, H. Wang, Z. Li and J. Li, *AICHE J*, 2013, **59**, 2195.

5 J. A. Mason, K. Sumida, Z. R. Herm, R. Krishna and J. R. Long, *Energy Environ. Sci.*, 2011, **4**, 3030.

6 A. Ö. Yazaydin, R. Q. Snurr, T.-H. Park, K. Koh, J. Liu, M. D. LeVan, A. I. Benin, P. Jakubczak, M. Lanuza, D. B. Galloway, J. L. Low and R. R. Willis, *J. Am. Chem. Soc.*, 2009, **131**, 18198.

7 P. D. C. Dietzel, V. Besikiotis and R. Blom, *J. Mater. Chem.*, 2009, **19**, 7362.

8 H. J. Park and M. P. Suh, *Chem. Sci.*, 2013, **4**, 685.

9 J. R. Li, J. M. Yu, W. G. Lu, L. B. Sun, J. Sculley, P. B. Balbuena and H. C. Zhou, *Nat. Commun.*, 2013, **4**, 1538.

10 J. McEwen, J. D. Hayman and A.O. Yazaydin, *Chem Phys*, 2013, **412**, 72.

11 R. V. Siriwardance, M. S. Shen, E. P. Fisher and J. A. Poston, *Energy Fuels*, 2001, **15**, 279.

12 W. Lu, D. Yuan, J. Sculley, D. Zhao, R. Krishna and H. C. Zhou, *J. Am. Chem. Soc.*, 2011, **133**, 18126.

13 F. Xiao, Z. Chen, G. Casillas, C. Richardson, H. Li and Z. Huang, *Chem. Comm.*, 2016, **52**, 3911.

14 S. Marchesini, C. M. McGilvery, J. Bailey and C. Petit, *ACS Nano*, 2017, **11**, 10003.

15 S. Marchesini, A. Regoutz, D. Payne and C. Petit, *Microporous Mesoporous Mater.*, 2017, **243**, 154.

16 X. Fan, L. Zhang, G. Zhang, Z. Shu and J. Shi, *Carbon*, 2013, **61**, 423.

17 M. Sevilla and A.B. Fuertes, *J. Colloid Interface Sci.*, 2012, **366**, 147.